Selective targeting of $\alpha_4\beta_7$/MAdCAM-1 axis suppresses liver fibrosis by reducing proinflammatory T cell recruitment to the liver

Biki Gupta[1]†, **Ravi Prakash Rai**[1]†, Pabitra B. Pal[1], Sudrishti Chaudhary[1], Anna Chiaro[1], Shannon Seaman[1], Aatur D. Singhi[2,3], Satdarshan P. Monga[1,2,4], Smita S. Iyer[1], Reben Raeman*[1,2]

†**Contributed equally**

[1]Division of Experimental Pathology, Department of Pathology, University of Pittsburgh, Pittsburgh, PA. [2]Pittsburgh Liver Research Center, University of Pittsburgh Medical Center and University of Pittsburgh School of Medicine, Pittsburgh, PA USA. [3]Division of Anatomic Pathology, Department of Pathology, University of Pittsburgh School of Medicine, Pittsburgh, PA USA. [4]Division of Gastroenterology, Hepatology and Nutrition, Department of Medicine, University of Pittsburgh School of Medicine, Pittsburgh, PA USA.

***Corresponding Author:**

Reben Raeman, M.S., Ph.D.

Assistant Professor

200 Lothrop Street, S408 BST,

Pittsburgh, PA 15261

Phone: 412-648-2021

Email: reben.raeman@pitt.edu

ABSTRACT

Integrin $\alpha_4\beta_7$+ T cells perpetuate tissue injury in chronic inflammatory diseases, yet their role in hepatic fibrosis progression remains poorly understood. Here we report increased accumulation of $\alpha_4\beta_7$+ T cells in the liver of people with cirrhosis relative to disease controls. Similarly, hepatic fibrosis in the established mouse model of CCl_4-induced liver fibrosis was associated with enrichment of intrahepatic $\alpha_4\beta_7$+ CD4 and CD8 T cells. Monoclonal antibody (mAb)-mediated blockade of $\alpha_4\beta_7$ or its ligand mucosal addressin cell adhesion molecule (MAdCAM)-1 attenuated hepatic inflammation and prevented fibrosis progression in CCl_4 treated mice. Improvement in liver fibrosis was associated with a significant decrease in the infiltration of $\alpha_4\beta_7$+ CD4 and CD8 T cells suggesting that $\alpha_4\beta_7$/MAdCAM-1 axis regulates both CD4 and CD8 T cell recruitment to the fibrotic liver, and $\alpha_4\beta_7$+ T cells promote hepatic fibrosis progression. Analysis of hepatic $\alpha_4\beta_7$+ and $\alpha_4\beta_7$- CD4 T cells revealed that $\alpha_4\beta_7$+ CD4 T cells enriched for markers of activation and proliferation demonstrating an effector phenotype. Notably, blockade of $\alpha_4\beta_7$ or MAdCAM-1 did not affect the recruitment of Foxp3+ regulatory T cells, demonstrating the specificity of $\alpha_4\beta_7$/MAdCAM-1 axis in regulating effector T cell recruitment to the liver. The findings suggest that $\alpha_4\beta_7$+ T cells play a critical role in promoting hepatic fibrosis progression, and mAb-mediated blockade of $\alpha_4\beta_7$ or MAdCAM-1 represents a promising therapeutic strategy for slowing hepatic fibrosis progression in chronic liver diseases.

INTRODUCTION

Wound healing and repair are fundamental biological processes critical to maintaining tissue architecture and restoring organ homeostasis following injury [1]. Protracted injury, however, can dysregulate this process resulting instead in excessive extracellular matrix deposition and tissue scarring or fibrosis. Progressive fibrosis is characteristic of advanced chronic liver diseases (CLDs), including alcoholic and nonalcoholic steatohepatitis as well as viral and autoimmune hepatitis[2-4]. Chronic unresolved fibrosis can lead to cirrhosis, the 11th leading cause of global deaths, and a major risk factor for developing hepatocellular carcinoma (HCC) which is among the top 20 causes of deaths worldwide. Consequently, therapeutic strategies to stop progression of fibrosis are urgently needed.

The inflammatory response to liver injury, essential for resolution of injury and tissue repair, is a highly regulated process where both the initiation and resolution of inflammation are mediated by the liver-resident and liver-recruited immune cells. Chronic injury, however, leads to a perpetuation of hepatic inflammation characterized by sustained infiltration of immune cells to the liver and maintenance of fibrogenic pathways. While the liver-resident macrophages or Kupffer cells (KC) play a key role in the initiation of inflammation, recent data show that they are depleted in the advanced stages of CLD. Ultimately, the recruited proinflammatory immune cells including cells of both myeloid and lymphoid origin play a more prominent role in fibrosis progression making them an interesting target for therapeutic approaches to address fibrosis progression [5].

Immune cell recruitment to the liver following injury is mediated by chemokines and cytokines released by damaged hepatocytes, activated KCs as well as HSC-derived myofibroblasts. Recently, we demonstrated that the heterodimeric integrin receptor $\alpha_4\beta_7$ expressed on T cells and its ligand, mucosal addressin cell adhesion molecule (MAdCAM)-1, expressed on endothelial cells, drive hepatic inflammation in NASH by promoting recruitment of $\alpha_4\beta_7$+ CD4 T cells to the liver [6]. The $\alpha_4\beta_7$/MAdCAM-1 axis is also implicated in promoting hepatic inflammation in chronic inflammatory liver diseases and primary sclerosing cholangitis (PSC), and upregulation of MAdCAM-1 expression is reported in the liver of most CLD patients [7-10]. Despite strong evidence suggesting that the $\alpha_4\beta_7$/MAdCAM-1 axis is influential in CLD, role of $\alpha_4\beta_7$/MAdCAM-1 axis in promoting hepatic fibrosis progression remain poorly delineated.

In the current study, using established model of CCl_4-induced liver fibrosis, we show a critical role of $\alpha_4\beta_7$+CD4 and $\alpha_4\beta_7$+CD8 T cells in promoting hepatic fibrosis progression. Our findings suggests that blocking $\alpha_4\beta_7$/MAdCAM-1-mediated recruitment of $\alpha_4\beta_7$+ T cells to the liver may represent a novel therapeutic strategy to slow or prevent fibrosis progression in CLD.

METHODS

Mice. Adult male C57BL/6J mice were obtained from The Jackson Laboratory (Bar Harbor, ME). The mice were maintained at the University of Pittsburgh Division of Animal Resources. Age- and sex-matched littermates were used for all experiments at 8–10 wk of age. All animal studies were carried out in accordance with protocols approved by the Institutional Animal Care and Use Committee at the University of Pittsburgh.

Mouse model of liver fibrosis and $\alpha_4\beta_7$ and MAdCAM-1 antibody treatment. To induce hepatic fibrosis, eight-week-old male mice were given twice-weekly oral gavage of CCl_4 (2 mL/Kg CCl_4 in 1:1 v/v olive oil) for six weeks. Mice receiving equal volume of olive oil served as vehicle controls. After 2 weeks of CCl_4 treatment, a cohort of mice were treated with twice weekly intraperitoneal injections of 8 mg/Kg $\alpha_4\beta_7$ mAb (DATK32; Bioxcell, West Lebanon, NH) or MAdCAM-1 mAb (MECA-367; Bioxcell, West Lebanon, NH) or rat IgG2a isotype antibody (Bioxcell, West Lebanon, NH) for four weeks.

Human tissue. De-identified, fixed explanted liver tissues from people receiving orthotopic liver transplantation for decompensated liver cirrhosis were obtained from Biospecimen Processing and Repository Core at Pittsburgh Liver Research Centre. Liver tissue from tumor-adjacent parenchyma of people with hepatocellular carcinoma was used as controls.

Histopathology. Histopathological analyses, including Hematoxylin and eosin (H&E) and Sirius Red staining, were conducted on formalin-fixed liver tissue sections as previously reported.[11] Photomicrographs of the histologic sections were obtained by using a Zeiss Light Microscope (Zeiss, Jena, Germany).

Immunofluorescence microscopy. Immunofluorescence (IF) microscopy was conducted on liver cryosections as previously reported.[11] The IF images were visualized and obtained by using an Axioskop 2 plus microscope (Zeiss, Jena, Germany). Following antibodies were used for mouse tissue, $\alpha_4\beta_7$/LPAM1(cat. No. 120702, Clone: MECA-367, Biolegend), aSMA (cat. No. MA1-06110, ThermoFisher Scientific), MAdCAM1(cat. No. 16-5997-85, ThermoFisher

Scientific). Following antibodies were used for human tissue, $\alpha_4\beta_7$/LPAM1(cat. No. DDX1434P-100, Clone: 11D9.03, Novus Biologicals) and CD3 (cat. No. ab135372, Abcam).

Serological analysis. Serum alanine aminotransferase (ALT), and aspartate aminotransferase (AST) concentrations were measured using an AST and ALT Activity Assay Kit (Sigma-Aldrich, St. Louis, MO).

Flow cytometric analysis. Livers perfused with 1X PBS (Thermo Fisher Scientific, Waltham, MA) were digested with 2mg/mL type IV collagenase (Worthington, NY) to obtain single cell suspensions and the lymphocytes were enriched by Percoll gradient centrifugation as describes previously [11]. Enriched lymphocytes were stained with fluorochrome-conjugated antibodies and fixable viability stain (BD Biosciences, San Jose, CA), and samples were acquired on Cytek Aurora Spectral Cytometer (Cytek Biosciences, Bethesda, MD) equipped with five lasers. Data were analyzed using FlowJo software v X.10 (Tree Star, Inc., Ashland, OR) as describes previously [11]. Total numbers were computed by multiplying proportion of specific populations to total numbers of enriched lymphocytes/liver. Fuorochrome conjugated antibodies against CD45 (30-F11), CD3 (17A2), CD4 (RM4-5), CD8 (53-6.7), CD44 (IM7), CD69 (H1.2F3), Tbet (4B10) and $\alpha_4\beta_7$ (LPAM-1; DATK32) were purchased from BD Biosciences (San Jose, CA), and Foxp3 (FJK-16s), Ki67 (SolA15) and Live/Dead Aqua was purchased form ThermoFisher Scientific (Waltham, MA).

Quantitative real-time PCR. Isolation of total RNA from liver, cDNA synthesis and qRT-PCR were performed as previously described.[11] Data were normalized to 18S rRNA and data are presented as fold change in gene expression compared to controls.

Statistical analysis. Two-tailed Student's t test was employed to compare mean differences between two groups. One-way ANOVA in conjunction with post-hoc analysis for multiple group comparison was employed to investigate statistical differences. A p value < 0.05 was considered statistically significant. Data shown are representative of 3 independent experiments. Statistical analyses were performed using GraphPad Prism 8.0 (GraphPad Software) software.

RESULTS

Integrin $\alpha_4\beta_7$ blockade attenuates CCl_4-induced hepatic inflammation. We recently demonstrated that blocking $\alpha_4\beta_7$+ T cell recruitment to the liver reduces hepatic injury in a murine model of NASH [6]. To determine whether $\alpha_4\beta_7$+ T cells play a role in promoting hepatic fibrosis, we used established mouse model of liver fibrosis to investigate whether blocking recruitment of $\alpha_4\beta_7$+ T cells would be effective in decreasing hepatic fibrosis progression (**Fig. 1A**). Mice were treated with CCl_4 for six weeks to induce hepatic fibrosis. Mice administered the vehicle olive oil served as controls. A cohort of CCl_4-treated mice received $\alpha_4\beta_7$ mAb for four weeks starting at week three. Mice treated with IgG isotype antibody served as controls (CCl_4 + IgG). As shown in **Fig. 1B**, CCl_4 + IgG-treated mice experienced severe liver injury indicated by increased infiltration of immune cells, steatosis and necrotic hepatocytes relative to vehicle controls. Increased liver injury in CCl_4 + IgG-treated mice was further corroborated by high serum aspartate aminotransferase (AST) and alanine aminotransferase (ALT) levels relative to

vehicle controls (**Fig. 1C-D**). Transcript levels of key pro-inflammatory cytokines, tumor necrosis factor-α (TNFα) and interleukin IL-6, were also significantly upregulated in the livers of CCl_4 + IgG- treated mice relative to controls indicative of severe hepatic inflammation (**Fig. 1E-F**). In contrast, histological analysis of liver tissue sections from CCl_4 + $\alpha_4\beta_7$-mAb-treated mice revealed substantial improvement in hepatic inflammation as evidenced by reduced infiltration of immune cells and reduced tissue injury (**Fig. 1B**). The marked attenuation of liver injury in CCl_4 + $\alpha_4\beta_7$-mAb treated mice was further substantiated by significantly reduced serum ALT and AST levels (**Fig. 1C-D**). Compared to IgG controls, $\alpha_4\beta_7$ mAb treatment also significantly reduced transcript levels of key pro-inflammatory cytokines, TNF-α and IL-6, in the liver (**Fig. 1E-F**). Collectively, these results demonstrate that $\alpha_4\beta_7$ blockade protected mice from CCl_4-induced hepatic inflammation and injury.

Integrin $\alpha_4\beta_7$ blockade reduces hepatic fibrosis progression. To determine the effect of $\alpha_4\beta_7$ blockade on hepatic fibrosis, liver tissue sections were stained with Sirius Red to assess collagen deposition while transcript levels of key molecules associated with hepatic fibrogenesis were quantified by qRT-PCR. As shown in **Fig. 2A**, CCl_4 treatment induced severe hepatic fibrosis indicated by increased collagen deposition in the livers of CCl_4 + IgG-treated mice compared to vehicle controls. The transcript levels of fibrogenesis marker α-smooth muscle actin (αSMA), a key marker of hepatic stellate cell (HSC) activation, collagen I (Col IA1 and Col IA2), transforming growth factor-β1 (TGF-β1), and tissue inhibitor of metalloproteinase-1 (TIMP-1) were also significantly elevated in the CCl_4 + IgG-treated mice relative to controls (**Fig. 2B-F**). Treatment with $\alpha_4\beta_7$ mAb reduced hepatic fibrosis reflected by decreased collagen deposition in the liver and significant reduction in the transcript levels of αSMA, Col IAI and Col IAII, TGF-

β1 and TIMP-1 (**Fig. 2A-F**). These results were further corroborated by confocal imaging of αSMA-stained liver tissue sections demonstrating significant inhibition of HSC activation evidenced by reduced hepatic αSMA-expressing HSCs following $\alpha_4\beta_7$ mAb treatment (**Fig. 2G**). Taken together, these results demonstrate that $\alpha_4\beta_7$ blockade attenuates CCl_4-induced hepatic fibrosis.

$\alpha_4\beta_7$ mAb treatment reduces accumulation of $\alpha_4\beta_7$+ T cells in the fibrotic liver. To determine whether α4β7 mAb treatment reduces hepatic inflammation and fibrosis in CCl4-treated mice by decreasing the recruitment of α4β7+ immune cells to the liver, we assessed hepatic immune cell infiltrates using flow cytometry. Phenotypic analysis of intrahepatic lymphocytes revealed significant enrichment of α4β7+ CD4 and CD8 T cells in the livers of CCl4 + IgG-treated mice compared to vehicle controls (**Fig. 3B-E**). Treatment with $\alpha_4\beta_7$ mAb significantly reduced intrahepatic $\alpha_4\beta_7$+ CD4 and CD8 T cells in CCl_4-treated mice compared to IgG controls (**Fig. 3B-E**). These findings were further supported by the significantly higher transcript levels of integrins α_4, β_7 and β_1 in the CCl4 + IgG-treated mice relative to vehicle controls (**Fig. 3F-H**). Treatment with $\alpha_4\beta_7$ mAb significantly reduced transcript levels of integrins α_4 and β_7, but not β_1, demonstrating the specificity of $\alpha_4\beta_7$ mAb in blocking the recruitment of $\alpha_4\beta_7$+ immune cells to the fibrotic liver (**Fig. 3F-H**). Colocalization studies also revealed increased infiltration of $\alpha_4\beta_7$+ CD4 and CD8 T cells in the livers of CCl_4 + IgG-treated mice relative to vehicle controls (**Fig. 3I-J**). Notably, treatment with $\alpha_4\beta_7$ mAb markedly decreased the infiltration of $\alpha_4\beta_7$+ CD4 and CD8 T cells in the liver relative to IgG-treated mice, demonstrating that $\alpha_4\beta_7$ blockade reduces $\alpha_4\beta_7$+ T cell recruitment to the fibrotic liver (**Fig. 3I-J)**. Collectively, these findings indicate that $\alpha_4\beta_7$ regulates recruitment and accumulation of CD4 and CD8 T cells in the fibrotic liver.

MAdCAM-1 blockade reduces CCl_4-induced hepatic infiltration of $\alpha_4\beta_7^+$ T cells. To determine if MAdCAM-1 blockade have a similar impact on hepatic $\alpha_4\beta_7$+ T cell recruitment in CCl_4-treated mice and ultimately attenuate liver injury, a cohort of the CCl_4-treated mice were treated with MAdCAM-1 mAb for four weeks. Mice treated with IgG isotype served as controls (**Fig. 4A)**. As shown in **Fig. 4B-E**, four weeks of MAdCAM-1 mAb treatment significantly decreased intrahepatic $\alpha_4\beta_7$+ CD4 and CD8 T cells in the CCl_4 + MAdCAM-1 mAb-treated mice relative to IgG controls. Treatment with MAdCAM-1 mAb did not impact the frequency but reduced the total number of Foxp3+ T regulatory cells (Tregs) in the liver (**Fig. 4F**). Analysis of intrahepatic innate immune cells revealed significant reduction in the frequency and the total number of macrophages (CD3-CD11b+Ly6G-F4/80+ cells) and monocytes (CD3-CD11b+Ly6G-Ly6C+ cells), but not neutrophils (CD3-CD11b+Ly6G+ cells), in the liver of CCl_4 + MAdCAM-1 mAb-treated mice relative to IgG controls (**Fig. 4G-I**). Treatment with MAdCAM-1 mAb significantly decreased the transcript levels of integrins α_4 and MAdCAM-1, but increased integrin β_7 transcripts, in the CCl_4-treated mice relative to IgG controls (**Fig. 4J-L**). These findings demonstrate that, similar to $\alpha_4\beta_7$, MAdCAM-1 blockade also reduces the recruitment of $\alpha_4\beta_7$+ T cells to the fibrotic liver, suggesting a role for the $\alpha_4\beta_7$/MAdCAM-1 axis in regulating $\alpha_4\beta_7$+ T cells to the fibrotic live.

$\alpha_4\beta_7$+ CD4 T cells enriched for markers of activation and proliferation demonstrating an effector phenotype. To determine the function of $\alpha_4\beta_7$+ CD4 T cells, we assessed the expression of T cell activation and proliferation markers in $\alpha_4\beta_7$ + and $\alpha_4\beta_7$ - CD4 T cell subsets in the liver of CCl_4 + IgG treated mice. Our analysis revealed that a significantly higher frequency of $\alpha_4\beta_7$+

CD4 T cells expressed the T cell activation marker CD44, acute T cells activation marker CD69, the Th1 transcriptional factor driving IFN production Tbet, and the cell proliferation marker Ki67 compared to the $\alpha_4\beta_7$- CD4 T cells (**Fig 5A-D**). These data suggest that $\alpha_4\beta_7$+ CD4 T cells comprise effector T cells with capacity for proliferation and cytokine production.

MAdCAM-1 blockade attenuates CCl_4-induced hepatic injury and fibrosis. Given the inhibitory effect of MAdCAM-1 blockade on the CCl_4-induced recruitment of immune cells to the liver, we examined whether MAdCAM-1 blockade reduced CCl_4-induced liver injury. Histological analysis of H&E-stained liver tissue sections revealed a notable decrease in hepatic inflammation and injury in CCl_4 + MAdCAM-1-mAb treated mice relative to the CCl_4 + IgG-treated mice (**Fig. 6A**). Improvement in hepatic injury in CCl_4 + MAdCAM-1-mAb treated mice was confirmed by decreased serum ALT levels (**Fig. 6B**). Treatment with MAdCAM-1-mAb significantly decreased the transcript levels of TGF-β and IL6, but not TNF-α (**Fig. 6C-E**). Treatment with MAdCAM-1 mAb decreased hepatic fibrosis indicated by marked decrease in the deposition of hepatic collagen in the Sirius Red-stained liver tissue sections (**Fig. 6F**). Transcript levels of key molecules associated with fibrogenesis of the liver, αSMA, TIMP-1, and Col IAI and Col IAII were significantly lower in the MAdCAM-1-mAb-treated mice relative to IgG controls (**Fig. 6G-J**). These data demonstrate that MAdCAM-1 blockade attenuates CCl_4-induced hepatic inflammation and fibrosis.

Increased infiltration of $\alpha_4\beta_7$+ T cells in the livers of NASH- and ASH-associated cirrhosis patients. To determine whether $\alpha_4\beta_7$+ T cells are also involved in the hepatic inflammation and fibrosis in people with end-stage liver disease, we probed liver tissue sections obtained from 10

people with NASH-associated cirrhosis and 10 people with ASH-associated cirrhosis for the presence of $\alpha_4\beta_7$+ T cells using confocal laser scanning microscopy. Liver tissue from tumor-adjacent parenchyma was used as controls. Staining of liver tissue sections with $\alpha_4\beta_7$ and CD3 antibodies revealed higher infiltration of $\alpha_4\beta_7$ and CD3 double-positive T cells and the formation of large inflammatory aggregates of $\alpha_4\beta_7$+ T cells in the livers of people with NASH- and ASH-associated cirrhosis (**Fig. 6K-L**). Interestingly, higher inflammatory aggregates of $\alpha_4\beta_7$+CD3+ T cells were observed in the fibrotic septa of livers from people with NASH-associated cirrhosis compared to those with ASH-associated cirrhosis. Collectively, these findings suggest the involvement of $\alpha_4\beta_7$+ T cells in people with end-stage liver disease.

DISCUSSION

Immune cells recruited to the injured liver are the primary instigators of sustained chronic inflammation and resulting fibrosis [12-15]; yet we lack complete understanding of the molecular mechanisms involved in immune-cell recruitment and the role of various immune cell subsets in promoting hepatic fibrosis. In this study, we report the involvement of the $\alpha_4\beta_7$/MAdCAM-1 axis in the recruitment of $\alpha_4\beta_7$+ T cells to the fibrotic liver, highlighting their pivotal role in promoting hepatic fibrosis progression. Using an established mouse model of liver fibrosis, we demonstrate the enrichment of $\alpha_4\beta_7$+ T cells in the fibrotic liver, and importantly, show that blocking $\alpha_4\beta_7$ or MAdCAM-1 reverses fibrosis progression by reducing the recruitment of $\alpha_4\beta_7$+ T cells to the liver. These findings unveil a previously unappreciated role for $\alpha_4\beta_7$+ T cells in promoting hepatic fibrosis progression.

Our clinical findings revealing the presence of inflammatory aggregates of $\alpha_4\beta_7$+ T cells in the livers of individuals with cirrhosis strongly indicate their involvement in liver injury. Furthermore, our data indicating larger inflammatory aggregates of $\alpha_4\beta_7$+ T cells in NASH-associated cirrhosis compared to ASH-associated cirrhosis suggest a potential heightened role of these cells in contributing to liver injury in NASH-associated cirrhosis. These findings, combined with previous reports on the $\alpha_4\beta_7$/MAdCAM-1 axis in regulating T cell recruitment in various CLDs, underscore the critical contribution of $\alpha_4\beta_7$+ T cells to hepatic inflammation and fibrosis progression in CLD [8,10,16,17].

Our findings from an established mouse model of liver fibrosis recapitulated our clinical findings by demonstrating that $\alpha_4\beta_7$+ T cells are actively recruited to the fibrotic liver and $\alpha_4\beta_7$+ T cells contribute to driving hepatic fibrosis progression in this model. Our results align with previous studies that reported protective effects against diet-induced non-alcoholic steatohepatitis (NASH) in mice lacking whole-body expression of MAdCAM-1 or treated with $\alpha_4\beta_7$ or MAdCAM-1 mAbs [6,18]. Additionally, whole-body knockout mice lacking MAdCAM-1 or β_7 have been shown to be protected from concavalin A-induced hepatitis [19]. In contrast, whole-body β_7 knockout mice have been shown to exhibit enhanced susceptibility to diet-induced NASH [18]. These discrepancies may be attributed to inherent defects in the development of gut-associated lymphoid tissue in β_7 knockout mice, making data interpretation more complex [20,21]. These conflicting findings also emphasize the limitations of relying solely on whole-body knockout mouse models in functional research, as non-specific phenotypes can often be overlooked. It should be noted that the $\alpha_4\beta_7$ mAb we used for our studies is a highly specific antibody that specifically binds to a conformational epitope accessible only in the $\alpha_4\beta_7$

heterodimer [22-24]. The specificity of this antibody has been extensively evaluated across various experimental and clinical contexts, and the humanized version of the $\alpha_4\beta_7$ monoclonal antibody has been recognized as an effective treatment for inflammatory bowel disease [23-26]. Furthermore, we demonstrate that treatment with MAdCAM-1 mAb also protects mice from CCl_4-induced liver fibrosis by blocking $\alpha_4\beta_7$+ T cell recruitment to the liver. These findings not only underscore the significance of the $\alpha_4\beta_7$/MAdCAM-1 axis in modulating T cell recruitment to the liver but also highlight the critical role played by $\alpha_4\beta_7$+ T cells in promoting hepatic fibrosis.

Our findings that $\alpha_4\beta_7$/MAdCAM-1 axis regulate CD4 T cell recruitment to the fibrotic liver adds to our previously reported role of this axis in regulating CD4 T cell recruitment to the NASH liver [6]. Consistent with earlier reports, our results confirmed that a significant proportion of $\alpha_4\beta_7$+ CD4 T cells are effector T cells [27,28]. Effector CD4 T cells are known to contribute to hepatic inflammation and fibrosis through the secretion of proinflammatory and profibrotic cytokines. Their activation leads to the stimulation of both innate and adaptive immune cells, thereby perpetuating the inflammatory and fibrotic processes within the liver [29-31]. In contrast, regulatory T cells expressing the transcription factor Foxp3 have been recognized for their ability to suppress immune responses and promote tissue repair [32]. In our study, we found that the $\alpha_4\beta_7$/MAdCAM-1 axis specifically targets the recruitment of $\alpha_4\beta_7$+ effector CD4 T cells to the fibrotic liver, while sparing the migration of Foxp3+ Tregs. This selectivity in blocking effector CD4 T cell recruitment while preserving the presence of immunomodulatory Tregs may have played a crucial role in the effectiveness of $\alpha_4\beta_7$ and MAdCAM-1 mAbs in suppressing hepatic fibrosis.

The involvement of CD8 T cells in tissue injury and fibrosis is of particular importance as antigen-specific or bystander activation of CD8 T cells can promote tissue injury by cytolysis of damaged cells or exacerbate inflammation by producing proinflammatory cytokines including TNF-α, INF-γ, IL-13, and IL-4 [33-37], which promote recruitment of proinflammatory immune cells to the injured tissue. Our data provide evidence supporting the role of the $\alpha_4\beta_7$/MAdCAM-1 axis in regulating the recruitment of CD8 T cells to the liver. Specifically, we demonstrate that a significant subset of CD8 T cells in the fibrotic liver express $\alpha_4\beta_7$. We demonstrate that blocking antibodies against $\alpha_4\beta_7$ and MAdCAM-1 that reduce recruitment of $\alpha_4\beta_7$+ CD8 T cells to the liver improves CCL_4-induced hepatic fibrosis. These findings expand upon the previously reported roles of the $\alpha_4\beta_7$/MAdCAM-1 axis in regulating CD4 T cell homing to the liver in NASH [6] and PSC [17]. Furthermore, our findings suggest that $\alpha_4\beta_7$-expressing CD8 T cells play a prominent role in promoting hepatic fibrosis in CLD. However, considering previous reports that CD8 T cells play a protective role during hepatic injury resolution by eliminating activated HSCs [38], and their dysfunction at the advanced stages of CLD exacerbate disease progression [39,40], further comprehensive investigations are needed to understand the specific functions of different CD8 T cell subsets in promoting and regressing hepatic fibrosis in CLD.

In conclusion, our findings shed light on the crucial role of the $\alpha_4\beta_7$/MAdCAM-1 axis in in regulating hepatic fibrosis and highlight the potential therapeutic strategy of utilizing mAbs targeting integrin $\alpha_4\beta_7$ or MAdCAM-1 to treat inflammation and fibrosis in CLD.

Data availability statement: Data sharing not applicable to this article as no datasets were generated or analyzed during the current study.

Conflict of interest: All authors declare no conflicting interests.

Author Contributions. Conceptualization: RR; Methodology: RR, SSI, BG, RPR, PBP, SC, AC, SS, ADS; Investigation: BG, SSI, RPR, PBP; Visualization: RR, BG, RPR, SSI, PBP; Funding acquisition: RR; Project administration: RR, BG, RPR; Supervision: RR; Writing – original draft: BG, RR; Writing – review & editing: RR, SSI, ADS, SPM.

Acknowledgements: Research reported in this publication was supported by the National Institute of Diabetes and Digestive and Kidney Diseases of the National Institutes of Health under award number K01DK110264 and R01DK124351 to RR; R01DK62277, R01DK100287 and Endowed Chair for Experimental Pathology to SPM; and R56AI150409 and RF1AG06001 to SSI. This research project was also supported in part by the University of Pittsburgh Clinical Biospecimen Processing and Repository Core and Advanced Cell and Tissue imaging Centre of the Pittsburgh Liver Research Centre supported by NIH/NIDDK Digestive Disease Research Core Center grant P30DK120531 and the University of Pittsburgh Unified Flow Core through the resources provided.

Keywords: Chronic liver disease; cirrhosis; T cells; fibrosis; inflammation

Short Title: $\alpha_4\beta_7$+ T cells promote hepatic fibrosis progression.

REFERENCES

1 Koyama, Y. & Brenner, D. A. Liver inflammation and fibrosis. *J Clin Invest* **127**, 55-64, doi:10.1172/JCI88881 (2017).

2 Lackner, C. & Tiniakos, D. Fibrosis and alcohol-related liver disease. *J Hepatol* **70**, 294-304, doi:10.1016/j.jhep.2018.12.003 (2019).

3 Alkhouri, N. & McCullough, A. J. Noninvasive Diagnosis of NASH and Liver Fibrosis Within the Spectrum of NAFLD. *Gastroenterol Hepatol (N Y)* **8**, 661-668 (2012).

4 Pinzani, M., Rombouts, K. & Colagrande, S. Fibrosis in chronic liver diseases: diagnosis and management. *J Hepatol* **42 Suppl**, S22-36, doi:10.1016/j.jhep.2004.12.008 (2005).

5 Wen, Y., Lambrecht, J., Ju, C. & Tacke, F. Hepatic macrophages in liver homeostasis and diseases-diversity, plasticity and therapeutic opportunities. *Cell Mol Immunol* **18**, 45-56, doi:10.1038/s41423-020-00558-8 (2021).

6 Rai, R. P. *et al.* Blocking integrin alpha4beta7-mediated CD4 T cell recruitment to the intestine and liver protects mice from western diet-induced non-alcoholic steatohepatitis. *J Hepatol*, doi:10.1016/j.jhep.2020.05.047 (2020).

7 Ala, A. *et al.* Mucosal addressin cell adhesion molecule (MAdCAM-1) expression is upregulated in the cirrhotic liver and immunolocalises to the peribiliary plexus and lymphoid aggregates. *Dig Dis Sci* **58**, 2528-2541, doi:10.1007/s10620-013-2755-1 (2013).

8 Grant, A. J., Lalor, P. F., Hubscher, S. G., Briskin, M. & Adams, D. H. MAdCAM-1 expressed in chronic inflammatory liver disease supports mucosal lymphocyte adhesion to hepatic endothelium (MAdCAM-1 in chronic inflammatory liver disease). *Hepatology* **33**, 1065-1072, doi:10.1053/jhep.2001.24231 (2001).

9 Borchers, A. T., Shimoda, S., Bowlus, C., Keen, C. L. & Gershwin, M. E. Lymphocyte recruitment and homing to the liver in primary biliary cirrhosis and primary sclerosing cholangitis. *Semin Immunopathol* **31**, 309-322, doi:10.1007/s00281-009-0167-2 (2009).

10 Graham, J. J. *et al.* Aberrant hepatic trafficking of gut-derived T cells is not specific to primary sclerosing cholangitis. *Hepatology* **75**, 518-530, doi:10.1002/hep.32193 (2022).

11 Rahman, K. *et al.* Loss of Junctional Adhesion Molecule A Promotes Severe Steatohepatitis in Mice on a Diet High in Saturated Fat, Fructose, and Cholesterol. *Gastroenterology* **151**, 733-746 e712, doi:10.1053/j.gastro.2016.06.022 (2016).

12 Karlmark, K. R., Wasmuth, H. E., Trautwein, C. & Tacke, F. Chemokine-directed immune cell infiltration in acute and chronic liver disease. *Expert Rev Gastroenterol Hepatol* **2**, 233-242, doi:10.1586/17474124.2.2.233 (2008).

13 Karlmark, K. R. *et al.* Hepatic recruitment of the inflammatory Gr1+ monocyte subset upon liver injury promotes hepatic fibrosis. *Hepatology* **50**, 261-274, doi:10.1002/hep.22950 (2009).

14 Pellicoro, A., Ramachandran, P., Iredale, J. P. & Fallowfield, J. A. Liver fibrosis and repair: immune regulation of wound healing in a solid organ. *Nat Rev Immunol* **14**, 181-194, doi:10.1038/nri3623 (2014).

15 Kisseleva, T. & Brenner, D. Molecular and cellular mechanisms of liver fibrosis and its regression. *Nat Rev Gastroenterol Hepatol* **18**, 151-166, doi:10.1038/s41575-020-00372-7 (2021).

16 Hillan, K. J. *et al.* Expression of the mucosal vascular addressin, MAdCAM-1, in inflammatory liver disease. *Liver* **19**, 509-518 (1999).

17 de Krijger, M., Wildenberg, M. E., de Jonge, W. J. & Ponsioen, C. Y. Return to sender: Lymphocyte trafficking mechanisms as contributors to primary sclerosing cholangitis. *J Hepatol* **71**, 603-615, doi:10.1016/j.jhep.2019.05.006 (2019).

18 Drescher, H. K. *et al.* beta7-Integrin and MAdCAM-1 play opposing roles during the development of non-alcoholic steatohepatitis. *J Hepatol* **66**, 1251-1264, doi:10.1016/j.jhep.2017.02.001 (2017).

19 Schippers, A. *et al.* MAdCAM-1/alpha4beta7 Integrin-Mediated Lymphocyte/Endothelium Interactions Exacerbate Acute Immune-Mediated Hepatitis in Mice. *Cell Mol Gastroenterol Hepatol* **11**, 1227-1250 e1221, doi:10.1016/j.jcmgh.2020.12.003 (2021).

20 Wagner, N. *et al.* Critical role for beta7 integrins in formation of the gut-associated lymphoid tissue. *Nature* **382**, 366-370, doi:10.1038/382366a0 (1996).

21 Sun, H. *et al.* Transmission of integrin beta7 transmembrane domain topology enables gut lymphoid tissue development. *J Cell Biol* **217**, 1453-1465, doi:10.1083/jcb.201707055 (2018).

22 Tidswell, M. *et al.* Structure-function analysis of the integrin beta 7 subunit: identification of domains involved in adhesion to MAdCAM-1. *J Immunol* **159**, 1497-1505 (1997).

23 Soler, D. *et al.* The binding specificity and selective antagonism of vedolizumab, an anti-alpha4beta7 integrin therapeutic antibody in development for inflammatory bowel diseases. *J Pharmacol Exp Ther* **330**, 864-875, doi:10.1124/jpet.109.153973 (2009).

24 Lazarovits, A. I. *et al.* Lymphocyte activation antigens. I. A monoclonal antibody, anti-Act I, defines a new late lymphocyte activation antigen. *J Immunol* **133**, 1857-1862 (1984).

25 Ley, K., Rivera-Nieves, J., Sandborn, W. J. & Shattil, S. Integrin-based therapeutics: biological basis, clinical use and new drugs. *Nat Rev Drug Discov* **15**, 173-183, doi:10.1038/nrd.2015.10 (2016).

26 Arijs, I. *et al.* Effect of vedolizumab (anti-alpha4beta7-integrin) therapy on histological healing and mucosal gene expression in patients with UC. *Gut* **67**, 43-52, doi:10.1136/gutjnl-2016-312293 (2018).

27 Wittner, M. *et al.* Comparison of the integrin alpha4beta7 expression pattern of memory T cell subsets in HIV infection and ulcerative colitis. *PLoS One* **14**, e0220008, doi:10.1371/journal.pone.0220008 (2019).

28 Kurmaeva, E. *et al.* T cell-associated α4β7 but not α4β1 integrin is required for the induction and perpetuation of chronic colitis. *Mucosal Immunol* **7**, 1354-1365, doi:10.1038/mi.2014.22 (2014).

29 Ramadori, P., Kam, S. & Heikenwalder, M. T cells: Friends and foes in NASH pathogenesis and hepatocarcinogenesis. *Hepatology* **75**, 1038-1049, doi:10.1002/hep.32336 (2022).

30 Chang, J. T., Wherry, E. J. & Goldrath, A. W. Molecular regulation of effector and memory T cell differentiation. *Nat Immunol* **15**, 1104-1115, doi:10.1038/ni.3031 (2014).

31 Lee, H. G., Cho, M. Z. & Choi, J. M. Bystander CD4(+) T cells: crossroads between innate and adaptive immunity. *Exp Mol Med* **52**, 1255-1263, doi:10.1038/s12276-020-00486-7 (2020).

32 Campbell, C. & Rudensky, A. Roles of Regulatory T Cells in Tissue Pathophysiology and Metabolism. *Cell Metab* **31**, 18-25, doi:10.1016/j.cmet.2019.09.010 (2020).

33 Neurath, M. F. Cytokines in inflammatory bowel disease. *Nat Rev Immunol* **14**, 329-342, doi:10.1038/nri3661 (2014).

34 Kopf, M., Bachmann, M. F. & Marsland, B. J. Averting inflammation by targeting the cytokine environment. *Nat Rev Drug Discov* **9**, 703-718, doi:10.1038/nrd2805 (2010).

35 Fuschiotti, P., Larregina, A. T., Ho, J., Feghali-Bostwick, C. & Medsger, T. A., Jr. Interleukin-13-producing CD8+ T cells mediate dermal fibrosis in patients with systemic sclerosis. *Arthritis Rheum* **65**, 236-246, doi:10.1002/art.37706 (2013).

36 Fuschiotti, P. Current perspectives on the role of CD8+ T cells in systemic sclerosis. *Immunol Lett* **195**, 55-60, doi:10.1016/j.imlet.2017.10.002 (2018).

37 Nakamura, K. *et al.* IL-4-producing CD8(+) T cells may be an immunological hallmark of chronic GVHD. *Bone Marrow Transplant* **36**, 639-647, doi:10.1038/sj.bmt.1705107 (2005).

38 Koda, Y. *et al.* CD8(+) tissue-resident memory T cells promote liver fibrosis resolution by inducing apoptosis of hepatic stellate cells. *Nat Commun* **12**, 4474, doi:10.1038/s41467-021-24734-0 (2021).

39 Ma, J. *et al.* PD1(Hi) CD8(+) T cells correlate with exhausted signature and poor clinical outcome in hepatocellular carcinoma. *J Immunother Cancer* **7**, 331, doi:10.1186/s40425-019-0814-7 (2019).

40 Collier, J. L., Weiss, S. A., Pauken, K. E., Sen, D. R. & Sharpe, A. H. Not-so-opposite ends of the spectrum: CD8(+) T cell dysfunction across chronic infection, cancer and autoimmunity. *Nat Immunol* **22**, 809-819, doi:10.1038/s41590-021-00949-7 (2021).

FIGURE LEGENDS

Figure 1. Integrin $\alpha_4\beta_7$ blockade attenuates CCl_4-induced hepatic inflammation. (**A**) Schematic of study design. Liver fibrosis was induced by oral administration of CCl_4 for six weeks. Mice treated with CCl_4 for six weeks received $\alpha_4\beta_7$ mAb or IgG isotype antibody for four weeks starting at week three. Mice administered the vehicle, olive oil, served as controls (n = 5 - 8 mice per group). (**B**) Representative photomicrographs of Hematoxylin and Eosin (H&E) stained liver tissue sections. (**C-D**) Serum AST and ALT levels. (**E-F**) Expression of key molecules associated with hepatic inflammation (n = 5 - 8 mice per cohort). Data are presented as mean ± SEM. Asterisks indicate significant differences ($p < 0.05$) between oil and IgG isotype control. Hashtags indicate significant differences ($p < 0.05$) between IgG and $\alpha_4\beta_7$ mAb treatments.

Figure 2. Integrin $\alpha_4\beta_7$ blockade attenuates CCl_4-induced hepatic fibrosis progression. (**A**) Representative photomicrographs of Sirius Red-stained liver tissue sections. Liver fibrosis was induced by oral administration of CCl_4 for six weeks. Mice treated with CCl_4 for six weeks received $\alpha_4\beta_7$ mAb or IgG isotype antibody for four weeks starting at week three. Mice administered the vehicle, olive oil, served as controls (n = 5 - 8 mice per group). (**B-F**) Expression of fibrosis markers in the liver. (**G**) Representative confocal images of αSMA (green) and DAPI (blue) immunofluorescence in the liver (n = 5 mice per group). Data are presented as mean ± SEM. Asterisks indicate significant differences ($p < 0.05$) between oil and IgG isotype

control. Hashtags indicate significant differences ($p < 0.05$) between IgG and $\alpha_4\beta_7$ mAb treatments.

Figure 3. Integrin $\alpha_4\beta_7$ mAb treatment reduces CCl_4-induced infiltration of $\alpha_4\beta_7$+ T cells in the liver. (**A**) Gating strategy used to identify intrahepatic lymphocytes. (**B-E**) Representative flow plots show percent of $\alpha_4\beta_7$+ CD4 and CD8 T cells, and bar graphs show percentage and total number of $\alpha_4\beta_7$+ CD4 and CD8 T cells in the liver. Mice treated with CCl_4 for six weeks received $\alpha_4\beta_7$ mAb or IgG isotype for four weeks starting at week three. Mice administered the vehicle, olive oil, served as controls (n = 5 - 8 mice per group). (**F-H**) Expression of integrins α_4, *Itga4*, β_7, *Itgb7* and β_1, *Itgb1* in the liver. (**I-J**) Representative confocal images of (**I**) $\alpha_4\beta_7$ (red) and CD4 (green) and (**J**) $\alpha_4\beta_7$ (red) and CD8 (green) immunofluorescence in the liver. Nuclei are stained with DAPI (blue). Data are presented as mean ± SEM. Asterisks indicate significant differences ($p < 0.05$) between oil and CCl_4 + IgG isotype controls. Hashtags indicate significant differences ($p < 0.05$) between IgG and $\alpha_4\beta_7$ mAb treatments.

Figure. 4. MAdCAM-1 blockade reduces CCL_4-induced infiltration of $\alpha_4\beta_7$+ T cells in the liver. (**A**) Schematic of study design. Mice treated with CCl_4 for six weeks received MAdCAM-1 mAb or IgG isotype antibody for four weeks starting at week three (n = 5 - 8 mice per cohort). (**B-E**) Representative flow plots show percent of $\alpha_4\beta_7$+ CD4 and CD8 T cells, and bar graphs show percentage and total number of $\alpha_4\beta_7$+ CD4 and CD8 T cells in the liver. (**F**) Percentage and total number of Foxp3+ CD4 T cells in the liver. (**G-I**) Percentage and total number of macrophages (CD3-CD11b+Ly6G-F4/80+ cells), monocytes (CD3-CD11b+Ly6G-Ly6C+ cells) and neutrophils (CD3-CD11b+Ly6G+ cells) in the liver. (**J-L**) Expression of integrins α_4, *Itga4*

and β_7, *Itga7* and *Madcam-1* in the liver (n = 5). Data are presented as mean ± SEM. Asterisks indicate significant differences ($p < 0.05$) between IgG and MAdCAM-1 mAb treatments.

Figure. 5. $\alpha_4\beta_7$+ CD4 T cells enriched for markers of activation and proliferation. demonstrating an effector phenotype. (**A**) Representative histograms show median fluorescence intensity of stated markers in the liver of mice treated with CCl_4 for six weeks. Gated on CD45+CD3+CD4+ cells. Mice were treated with IgG during the final four weeks (n = 5). Bar graphs show percentage of $\alpha_4\beta_7$+ and $\alpha_4\beta_7$- CD4 T cells expressing (**B**) T cell activation markers CD44 and CD69, (**C**) Th1 cell marker Tbet and (**D**) proliferation marker Ki67 in the liver. Data are presented as mean ± SEM. Asterisks indicate significant differences ($p < 0.05$) between $\alpha_4\beta_7$+ and $\alpha_4\beta_7$- CD4 T cells.

Figure. 6. MAdCAM-1 blockade attenuates hepatic inflammation and fibrosis progression. (**A**) Representative photomicrographs of Hematoxylin and Eosin (H&E) stained liver tissue sections. Mice treated with CCl_4 for six weeks received MAdCAM-1 mAb or IgG isotype antibody for four weeks starting at week three (n = 5 - 8 mice per group). (**B**) Serum ALT level. (**C-E**) Expression of key molecules associated with hepatic inflammation (n = 5- 8 mice per group). (**F**) Representative photomicrographs of Sirius Red-stained liver tissue sections. (**G-J**) Expression of key fibrosis markers in the liver. Data are presented as mean ± SEM. Hashtags indicate significant differences ($p < 0.05$) between IgG and MAdCAM-1 mAb treatments. (**K**) Representative photomicrographs of Sirius Red-stained liver liver tissue sections from disease controls and people with nonalcoholic steatohepatitis (NASH) and alcoholic steatohepatitis (ASH)-associated cirrhosis. (**L**) Representative confocal images of CD3 (red), α4β7 (green) and

DAPI (blue) immunofluorescence in the liver tissue sections. Insets show zoomed-in view of the region in white dotted box. White arrowheads, CD3 T cells. Yellow arrowheads, $\alpha_4\beta_7$+ CD3 T cells.

FIGURES

Figure 1

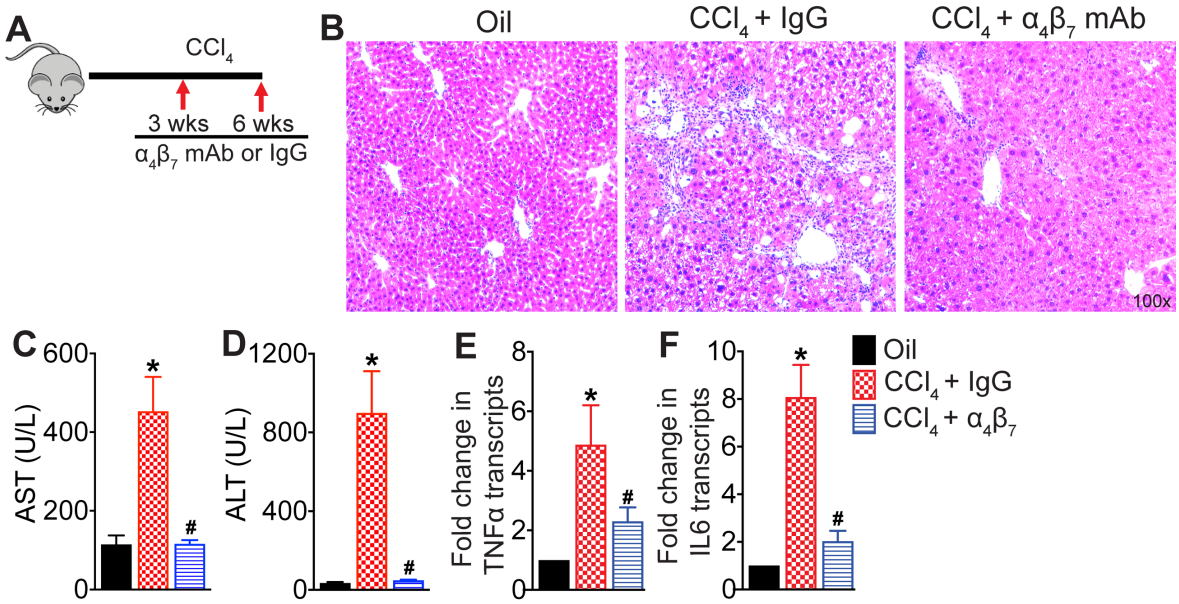

Figure 2

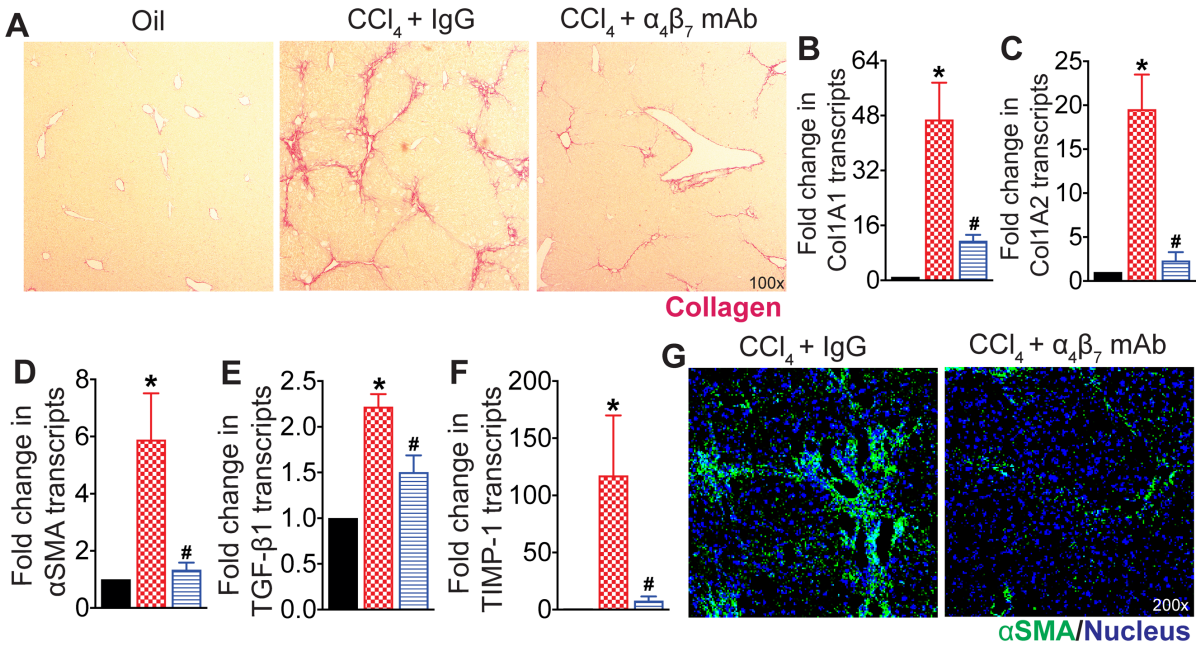
A
Oil
CCl4 + IgG
CCl4 + α4β7 mAb
100x
Collagen
B
Fold change in Col1A1 transcripts
64
48
32
16
0
*
#
C
Fold change in Col1A2 transcripts
25
20
15
10
5
0
*
#
D
Fold change in αSMA transcripts
8
6
4
2
0
*
#
E
Fold change in TGF-β1 transcripts
2.5
2.0
1.5
1.0
0.5
0.0
*
#
F
Fold change in TIMP-1 transcripts
200
150
100
50
0
*
#
G
CCl4 + IgG
CCl4 + α4β7 mAb
200x
αSMA/Nucleus

Figure 3

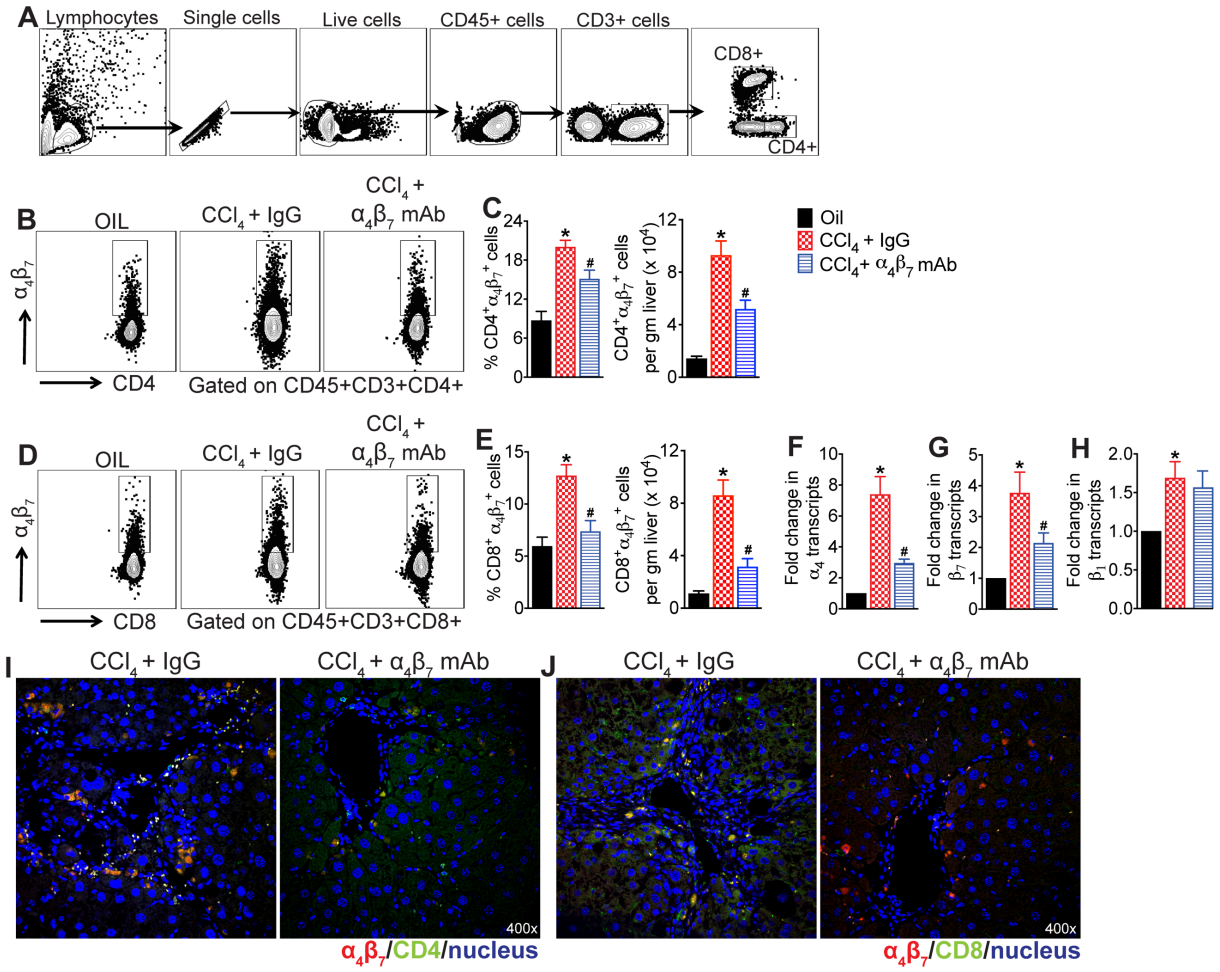
A
Lymphocytes
Single cells
Live cells
CD45+ cells
CD3+ cells
CD8+
CD4+
B
OIL
CCl4 + IgG
CCl4 + α4β7 mAb
α4β7
CD4
Gated on CD45+CD3+CD4+
C
% CD4+α4β7+ cells
CD4+α4β7+ cells per gm liver (x 10^4)
Oil
CCl4 + IgG
CCl4+ α4β7 mAb
D
OIL
CCl4 + IgG
CCl4 + α4β7 mAb
α4β7
CD8
Gated on CD45+CD3+CD8+
E
% CD8+ α4β7+ cells
CD8+α4β7+ cells per gm liver (x 10^4)
F
Fold change in α4 transcripts
G
Fold change in β7 transcripts
H
Fold change in β1 transcripts
I
CCl4 + IgG
CCl4 + α4β7 mAb
400x
α4β7/CD4/nucleus
J
CCl4 + IgG
CCl4 + α4β7 mAb
400x
α4β7/CD8/nucleus

Figure 4

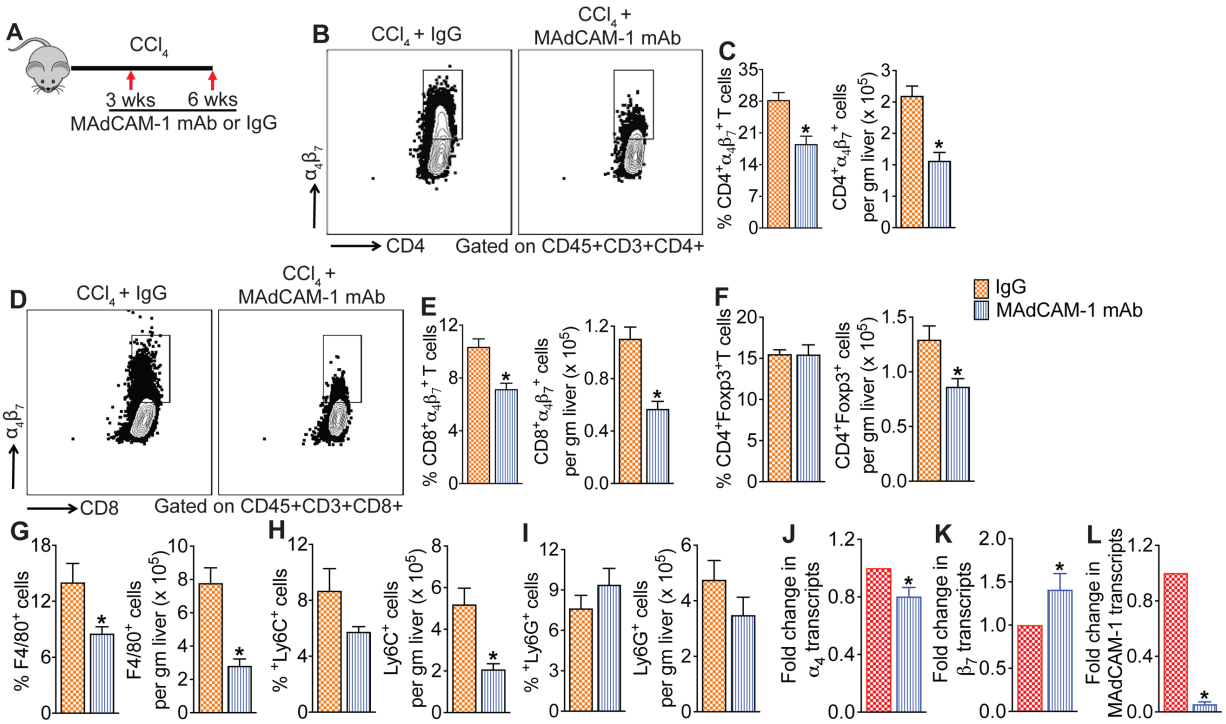
A
CCl4
3 wks
6 wks
MAdCAM-1 mAb or IgG
B
CCl4 + IgG
CCl4 + MAdCAM-1 mAb
α4β7
CD4
Gated on CD45+CD3+CD4+
C
% CD4+α4β7+ T cells
CD4+α4β7+ cells per gm liver (x 10^5)
D
CCl4 + IgG
CCl4 + MAdCAM-1 mAb
α4β7
CD8
Gated on CD45+CD3+CD8+
E
% CD8+α4β7+ T cells
CD8+α4β7+ cells per gm liver (x 10^5)
F
% CD4+Foxp3+T cells
CD4+Foxp3+ cells per gm liver (x 10^5)
IgG
MAdCAM-1 mAb
G
% F4/80+ cells
F4/80+ cells per gm liver (x 10^5)
H
% +Ly6C+ cells
Ly6C+ cells per gm liver (x 10^5)
I
% +Ly6G+ cells
Ly6G+ cells per gm liver (x 10^5)
J
Fold change in α4 transcripts
K
Fold change in β7 transcripts
L
Fold change in MAdCAM-1 transcripts

Figure 5

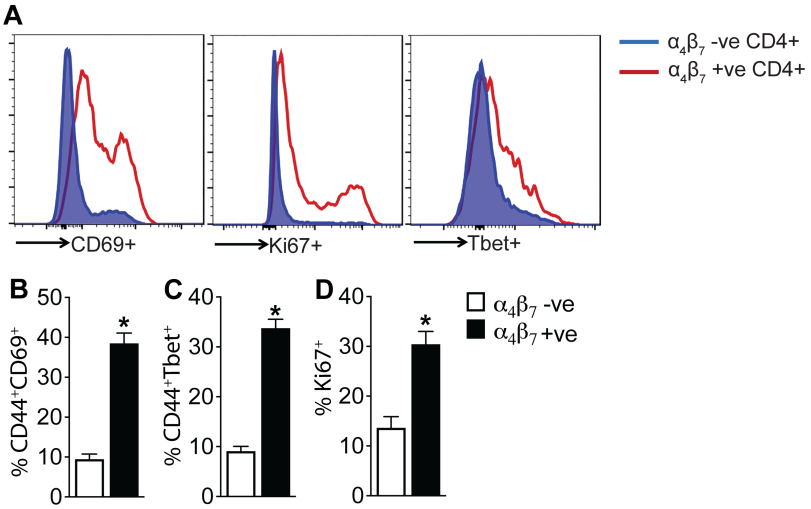
A
α4β7 -ve CD4+
α4β7 +ve CD4+
CD69+
Ki67+
Tbet+
B
% CD44+CD69+
C
% CD44+Tbet+
D
% Ki67+
α4β7 -ve
α4β7 +ve
*

Figure 6

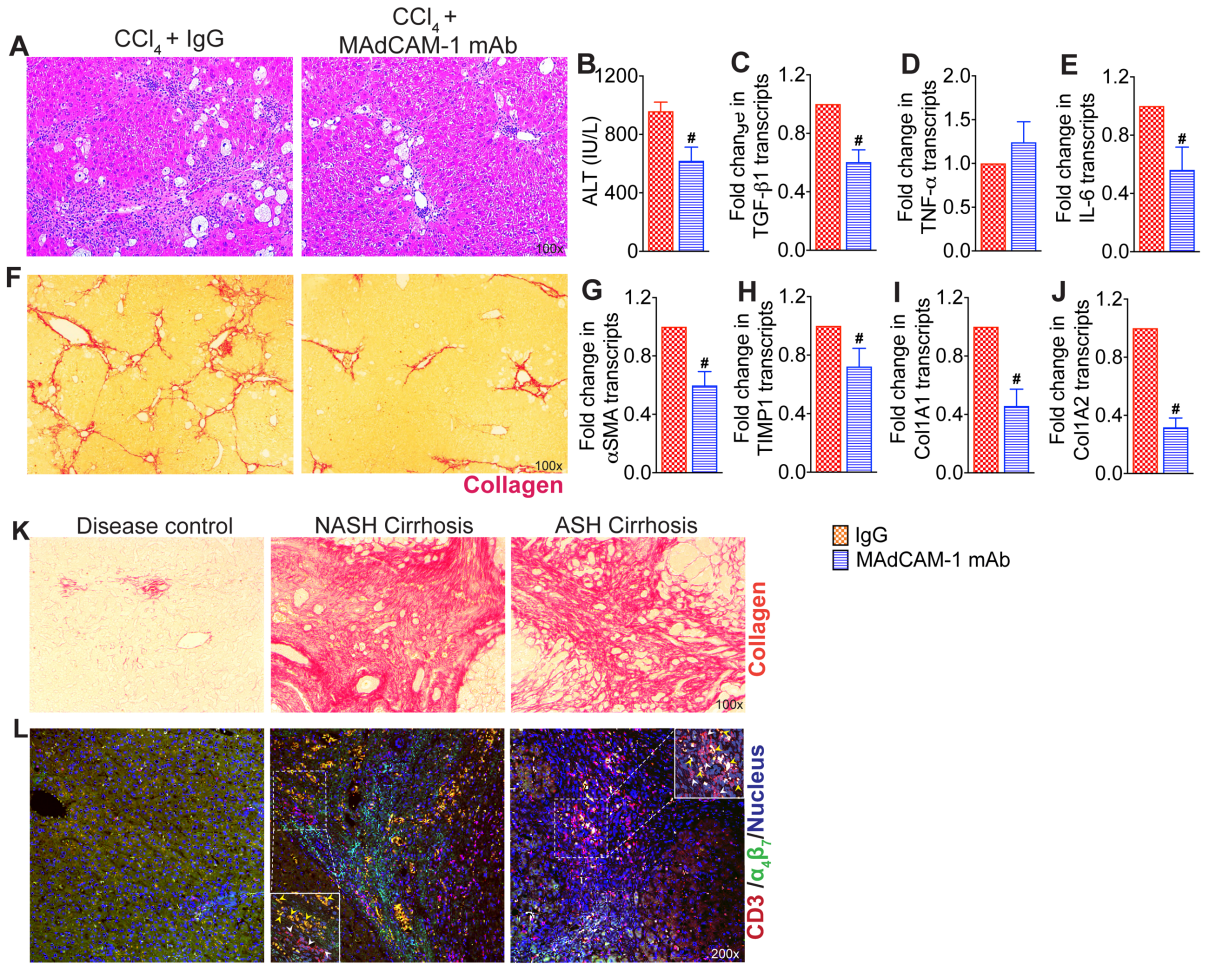
A
CCl4 + IgG
CCl4 + MAdCAM-1 mAb
100x
B
ALT (IU/L)
C
Fold change in TGF-β1 transcripts
D
Fold change in TNF-α transcripts
E
Fold change in IL-6 transcripts
F
Collagen
G
Fold change in αSMA transcripts
H
Fold change in TIMP1 transcripts
I
Fold change in Col1A1 transcripts
J
Fold change in Col1A2 transcripts
K
Disease control
NASH Cirrhosis
ASH Cirrhosis
Collagen
L
CD3 /α4β7/Nucleus
200x
IgG
MAdCAM-1 mAb